

**Slovak University of Technology in Bratislava
Institute of Information Engineering, Automation, and Mathematics**

PROCEEDINGS

of the 18th International Conference on Process Control

Hotel Titris, Tatranská Lomnica, Slovakia, June 14 – 17, 2011

ISBN 978-80-227-3517-9

<http://www.kirp.chtf.stuba.sk/pc11>

Editors: M. Fikar and M. Kvasnica

Kardoš, J.: The Robust Motion Control of a Robot Manipulator, Editors: Fikar, M., Kvasnica, M., In *Proceedings of the 18th International Conference on Process Control*, Tatranská Lomnica, Slovakia, 571–576, 2011.

Full paper online: <http://www.kirp.chtf.stuba.sk/pc11/data/abstracts/013.html>

The robust motion control of a robot manipulator

J. Kardoš *

* Faculty of Electrical Engineering and Information Technology, Slovak Univ. of Technology,
Ilkovičova 3, 812 19 Bratislava, Slovak Republic
(Tel: +421-2-6029-1776; e-mail: jan.kardos@stuba.sk)

Abstract: The contribution presents a verification of the fast and chattering-free robust variable structure fixed-target position control of the 2-DOF robot manipulator considering both the mutual interaction between the links and the gravitational forces influence as the signal disturbances. Numerical simulations in the joint space show the feasibility and effectiveness of the provided algorithm in the control of a complex mechatronic system.

1. INTRODUCTION

Any feasible control of the multi-DOF mechatronic system has to face the problem of an extreme variability of the plant parameters as well as a strong influence of the variable external forces (gravitational, Coriolis and centrifugal). The classical control methods are not able to manage satisfactory such a complex and difficult task at all. One of the promising control approaches is the contemporary variable structure control (VSC) theory with its specific and unique attribute – the sliding mode (sliding mode control – SMC) (Utkin et al. 1999), (Utkin 2002), (Kardoš 2009). The basic feature of the sliding mode is the high frequency oscillation of the actuating variable because of the switching principle in the control algorithm. In sliding mode, the system's phase trajectory is robust and independent of the parametric and external disturbances due to reserve in power.

Based on the VSC, the equivalent time sub-optimal control (ETSC) algorithm has been formulated for a single-DOF motion control system (Kardoš 2005). The main benefits of this control are a simple control structure, the fastest possible and overshoot-free response and the insensitivity to any (parametric and/or signal) type of disturbances. One of the problems of SMC, the chattering elimination, has been solved via the reaching law approach (Hung et al. 1993). The aim of this contribution is the implementation of the prospective ETSC algorithm in the control structure of a multi-DOF robot manipulator. Using the Euler-Lagrange formalism, a dynamic model of the robot manipulator has been derived (Kardoš 2010). For the purposes of this paper, the reduced model of a 2-DOF manipulator has been considered without loss of generality.

2. THE OUTLINE OF THE CONTROL ALGORITHM

The goal of the original time sub-optimal control (TSC) algorithm (Kardoš 2007) is the fast and overshoot-free positioning of the motion control system despite its variable dynamics. Let for the basic model of the generalized position

q generator given in the phase space (e, \dot{e}) by the system of the differential equations

$$\begin{aligned} \frac{de}{dt} &= \dot{e} \\ \frac{d\dot{e}}{dt} &= -\frac{1}{T}(Ku + \dot{e}) \end{aligned} \quad (1)$$

the time sub-optimal control be described by the group of expressions

$$\begin{aligned} u &= M \operatorname{sgn}(F(\mathbf{e})) \\ F(\mathbf{e}) &= \dot{e} + \alpha e \\ \alpha &= \frac{1}{T_{\max}(1 - \ln 2)} \end{aligned} \quad (2)$$

In (1) and (2), $e = q_d - q$ stands for the control error (q_d – desired position value), $\mathbf{e} = (e, \dot{e})^T$ corresponds to the system's error vector (the phase vector), $F(\mathbf{e})$ represents the linear switching function (a switching line with the slope α), u is the system's input (the control), $M > 0$ refers to the value of a natural limitation of the control u , K stands for the control channel gain and the time constant T represents the dominant variable parameter

$$T \in \langle T_{\min}, T_{\max} \rangle \quad (3)$$

Note that control (2) belongs to the switching type (discontinuous) VSC algorithms and that the majority of VSC prefers the linear switching function with its simple computation and realization. To avoid the chattering problem in a motion control system (the chattering denotes a low

frequency oscillation of system variables in sliding mode due to presence of parasitic dynamics and non-linearities in real mechatronic systems), the reaching law modification of the original control algorithm (2) has been performed (Kardoš 2005). The main idea of the reaching law is to force the system's state (the representative point in the phase portrait) to reach the switching function using the prescription given by the differential equation

$$\frac{dF(\mathbf{e})}{dt} = -kF(\mathbf{e}) \quad (4)$$

where $1/k$ represents the time constant of the switching function exponential evolution (decrease). Equation (4) meets the sliding mode existence condition (Utkin et al. 1999) and assures the chattering elimination replacing the discontinuous control by its smooth equivalent (close to mean value) in the vicinity of the switching function. Assuming the non-oscillating behaviour of the controlled variable q , using (1) and (2), we obtain a linear continuous equivalent control u_{EQU}

$$u_{EQU} = \frac{1}{K} \left[kT_{\max} \dot{e} + \frac{1}{1 - \ln 2} (\dot{e} \ln 2 + ke) \right] \quad (5)$$

Combining equation (5) with the control u limitation ($\text{abs}(u) \leq M$) in (2) yields the resultant equivalent time sub-optimal control (ETSC) (Kardoš 2005) in the form

$$u_{ETSC} = \begin{cases} u_{EQU} & \text{for } \text{abs}(u_{EQU}) < M \\ M \text{sgn}(u_{EQU}) & \text{for } \text{abs}(u_{EQU}) \geq M \end{cases} \quad (6)$$

The recommended value of parameter k

$$\begin{aligned} k &\gg 1 \\ k &\gg \alpha \end{aligned} \quad (7)$$

corresponds with the requirement of the fast and accurate control.

Algorithm (6) guarantees the robust and near-to-time optimal control of a single-DOF mechatronic system (SISO) (1) with the parametric uncertainty (3) in time constant (Kardoš 2005), (Kardoš 2007) as well as the chattering elimination in control structure (Kardoš 2005), which implies the low energy consumption. Furthermore, it is evident that signals necessary for the control algorithm completion, i.e. the position signal and the velocity one (cf. (5)), are in mechatronic systems directly accessible.

3. CONTROL OF THE ROBOT MANIPULATOR

The implementation of the proposed control strategy in the robot manipulator positioning control requires the thorough analysis of both the mutual interaction among the manipulator's degrees of freedom and the interaction between any DOF and the environment (e.g. the friction, the influence of the gravitation etc). Due to robustness of the presented control algorithm, such an interaction can be viewed as the signal disturbance. Consequently, the robot manipulator representing a complex MIMO system can be decoupled to a set of SISO systems, one for each DOF. Thus, any DOF can be controlled by its individual control algorithm (6).

Based on the Euler-Lagrange formalism, let the robot manipulator's dynamics be described by the matrix differential equation (Kardoš 2010)

$$\mathbf{J}(\mathbf{q})\ddot{\mathbf{q}} = \boldsymbol{\tau} - \mathbf{B}\dot{\mathbf{q}} - \mathbf{c}(\mathbf{q}, \dot{\mathbf{q}}) - \mathbf{g}(\mathbf{q}) \quad (8)$$

where \mathbf{q} and $\boldsymbol{\tau}$ stand for the vectors of generalized coordinates and generalized driving forces or torques respectively, $\mathbf{J}(\cdot)$ represents the inertia matrix, \mathbf{B} denotes the diagonal matrix of viscous friction coefficients, $\mathbf{c}(\cdot)$ corresponds to the vector of Coriolis and centrifugal forces and $\mathbf{g}(\cdot)$ stands for the vector of gravitational forces.

To keep the controllability of the manipulator DOF's, for the i^{th} DOF, the limitation M_i of the control u_i (in this particular case a limitation of the driving torque τ_i as an element of the driving forces vector $\boldsymbol{\tau}$) in the corresponding ETSC algorithm (6) should satisfy the condition

$$M_i \geq \max \left\{ B_i \dot{q}_i + c_i(\mathbf{q}, \dot{\mathbf{q}}) + g_i(\mathbf{q}) + \sum_j J_{ij}(\mathbf{q}) \ddot{q}_j \right\} \quad (9)$$

where B_i , c_i , g_i , J_{ij} , \dot{q}_i and \ddot{q}_j are the elements of the related matrices or vectors in (8). Note, that the values of elements in matrix \mathbf{J} as well as the ones in vectors \mathbf{c} and \mathbf{g} are extremely variable for the period of the robot positioning, which makes the utilization of conventional control theory methods almost impossible. To get the values of the control boundary M_i , the maximal values of both the joint angular acceleration and the joint angular velocity should be known. These values are given by the particular industrial technology where the controlled robot manipulator is supposed to be utilized. Taking into consideration the requirement of the fastest possible motion as well as the boundaries of acceleration and velocity, the command (desired value q_{di}) in high-quality controllable robot positioning should have the form of S-curve.

For the control purposes, after the decoupling of the original controlled plant (8), the values of the i^{th} DOF parameters are given by the pair of expressions

$$K_i = \frac{1}{B_i}$$

$$T_{i\max} = \frac{j_{ii\max}}{B_i} \tag{10}$$

4. EXPERIMENTAL RESULTS

The provided control algorithm has been applied in a numerical model of the robot manipulator control. A corresponding kinematic structure of the two-link manipulator is depicted in Figure 1, with the positive orientation of joint variables q_i ($i = 1, 2$) indicated by arrows. Both the controlled manipulator and the control algorithm parameters are given in Table 1. The resultant control structure in Matlab-Simulink can be seen in Figure 2.

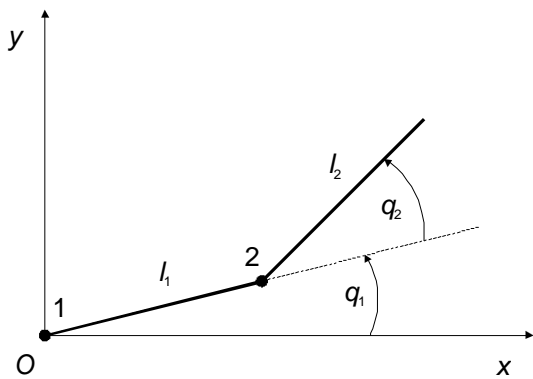


Fig. 1. Kinematic structure of the two-link manipulator

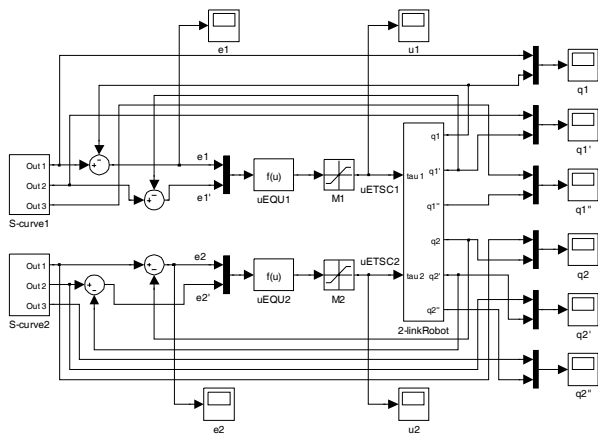


Fig. 2. Diagram of the Matlab control structure

The dynamic parameters of the robot endpoint trajectory (in the task space) equivalent to the angular values in the joint space are as follows: the maximal value of the acceleration $a_{\max} = 1.767\text{ms}^{-2}$, the maximal value of the velocity $v_{\max} = 1.767\text{ms}^{-1}$. Such parameters represent a sufficiently dynamic motion in robotized technologies, particularly in mechatronic systems with a strong coupling between the DOF's and with extremely variable time constants (proportional to the square of the varying distance between the revolute joint and the gravity centre of any rotating mass).

| Parameter | Joint number i | |
|--|------------------|--------|
| | 1 | 2 |
| Length l_i of a link [m] | 0.75 | 0.75 |
| Total mass m_i of a link [kg] | 30 | 32 |
| Coefficient of the viscous friction B_i [kgms ⁻¹] | 2 | 2 |
| Control channel gain K_i | 0.5 | 0.5 |
| Max. value of the moment of inertia $j_{ii\max}$ [kgm ²] | 88.875 | 18 |
| Max. value of the system's time constant $T_{i\max}$ [s] | 44.4375 | 9 |
| Joint angular velocity boundary $\dot{q}_{i\max}$ [rads ⁻¹] | 0.7854 | 0.7854 |
| Joint angular acceleration boundary $\ddot{q}_{i\max}$ [rads ⁻²] | 0.7854 | 0.7854 |
| Driving torque (control) boundary M_i [Nm] | 840 | 300 |
| Control parameter α_i (2) | 0.0733 | 0.3621 |
| Control parameter k_i (5) | 10000 | 10000 |

Tab. 1. Parameters of the 2-DOF robot control

Figures 3 to 8 show the control system behaviour in the time domain for a period of positioning between the starting position $q_1 = q_2 = 0$ and the target one $q_1 = q_2 = \pi/2$ (in radians) in both joints. The left column of figures corresponds to the first link of the manipulator, the right column to the second one. The perfect accuracy of positioning is evident in Figures 3 and 6, where the desired (S-curve) angular position q_{di} ($i = 1, 2$) and the controlled position q_i are depicted. The perfect tracking performance is assured by the high value of parameter k in (5). The related trapezoidal plots of the desired angular velocity \dot{q}_{di} and the output velocity \dot{q}_i in Figures 5 and 8 show the accuracy and robustness of the ETSC algorithm. In Figures 4 and 7 there is a time history of the driving torques τ_i in manipulator joints. The discontinuities in plots correspond with the intentional discontinuities in the motion acceleration. Neither of the driving torques exceeds the prescribed limitation M_i defined by (9) (cf. Table 1). A non-zero value of the driving torque in steady state represents in both joints the reaction of the driving force to the gravitational one (the second link is in a horizontal position).

To prove the robustness of the proposed control despite the significant coupling between the DOF's, a simulation with the constant mutual position of the robot links has been performed. Figures 9 to 14 show the system variables versus time plots in the case of the maximally stretched manipulator arm ($q_2 = 0$) during the whole period of motion (the initial angular position of the first link $q_1 = 0$, the target position $q_1 = \pi/2$). Again, the perfect accuracy and robustness of the proposed control is illustrated in Figures 9 and 12 with the angular position in the time domain. The stretched arm of the manipulator matches with the zero value of the angular position q_2 . A minimal difference between the desired and the actual angular position of the second link can be seen in Figure 14 with the 900-times enlarged scale of the vertical axis.

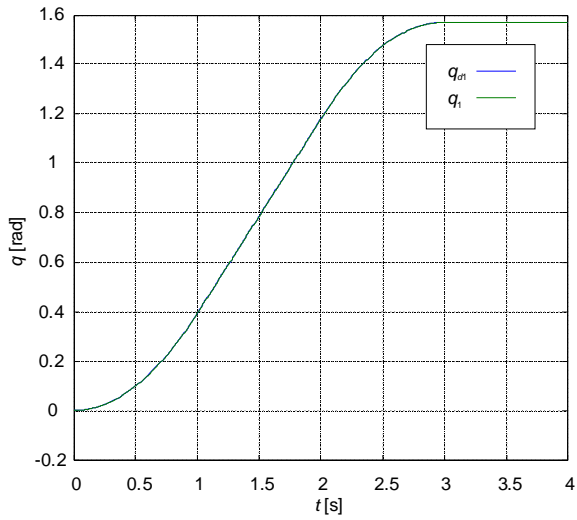


Fig. 3. First link: desired position q_{d1} and link position q_1

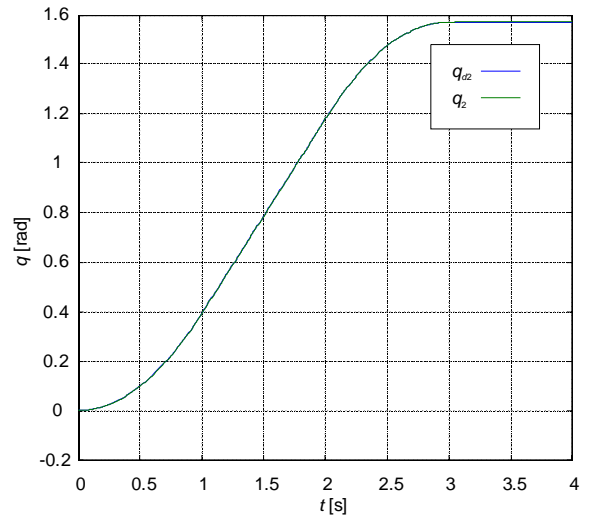


Fig. 6. Second link: desired position q_{d2} and link position q_2

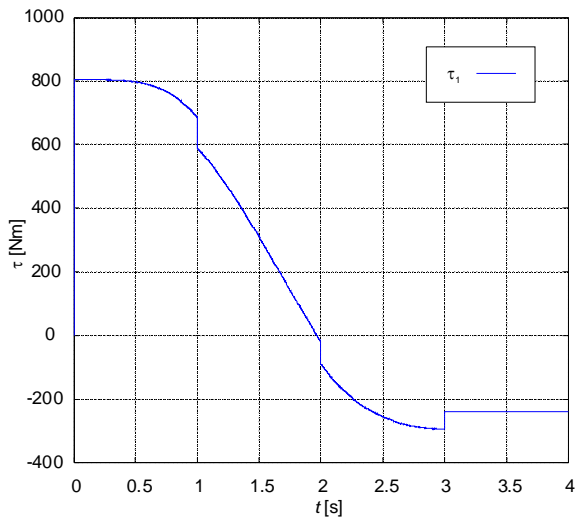


Fig. 4. First link: driving torque τ_1

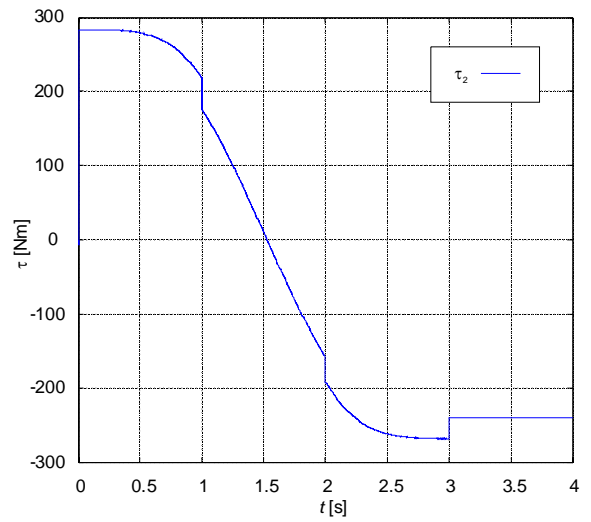


Fig. 7. Second link: driving torque τ_2

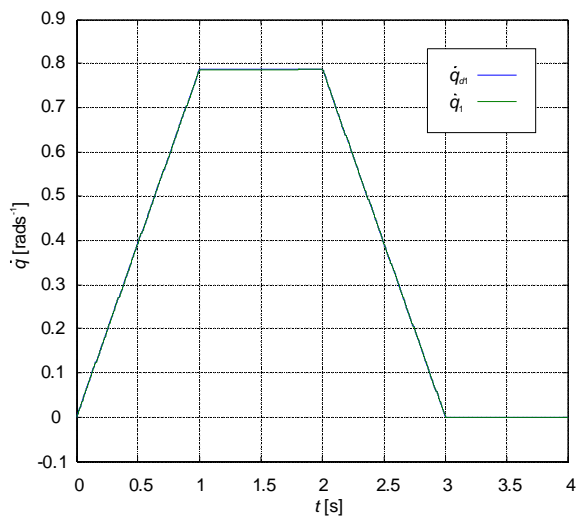


Fig. 5. First link: desired angular velocity \dot{q}_{d1} and link angular velocity \dot{q}_1

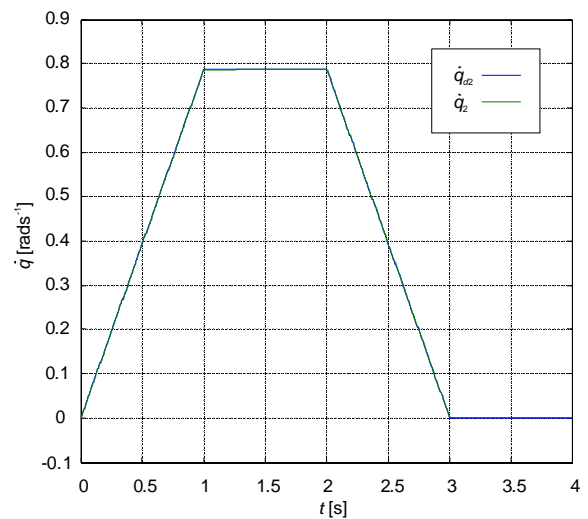


Fig. 8. Second link: desired angular velocity \dot{q}_{d2} and link angular velocity \dot{q}_2

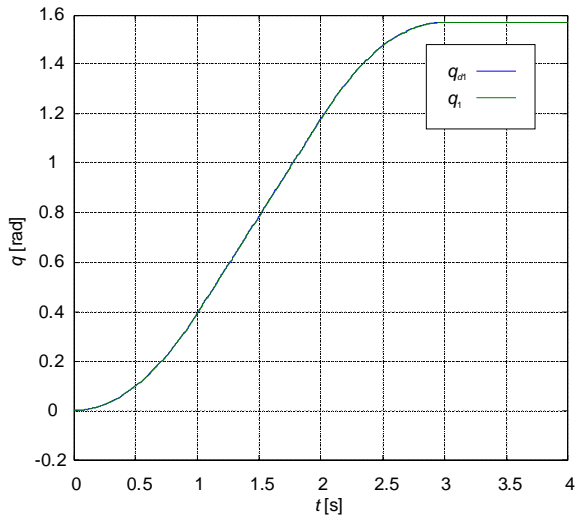


Fig. 9. First link, stretched arm: desired position q_{d1} and link position q_1

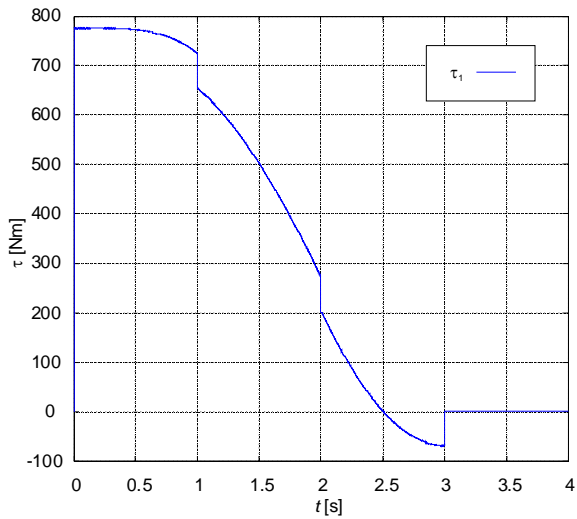


Fig. 10. First link, stretched arm: driving torque τ_1

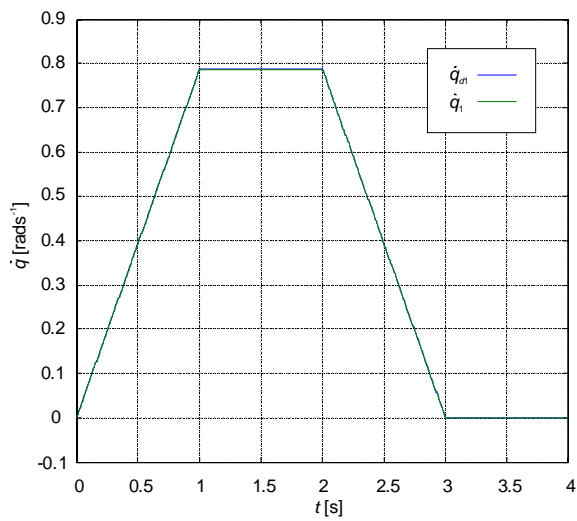


Fig. 11. First link, stretched arm: desired angular velocity \dot{q}_{d1} and link angular velocity \dot{q}_1

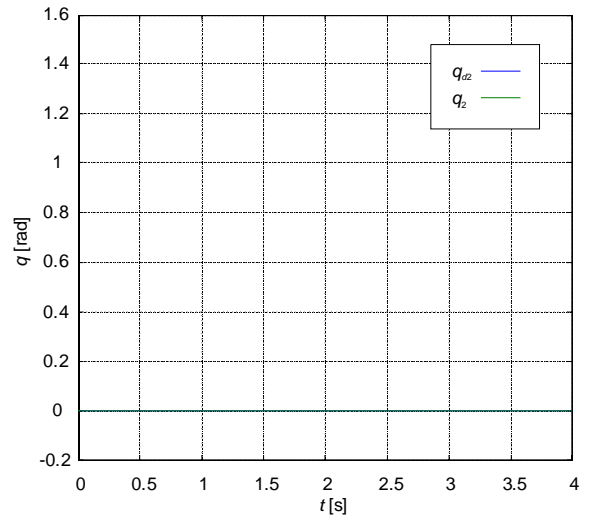


Fig. 12. Second link, stretched arm: desired position q_{d2} and link position q_2

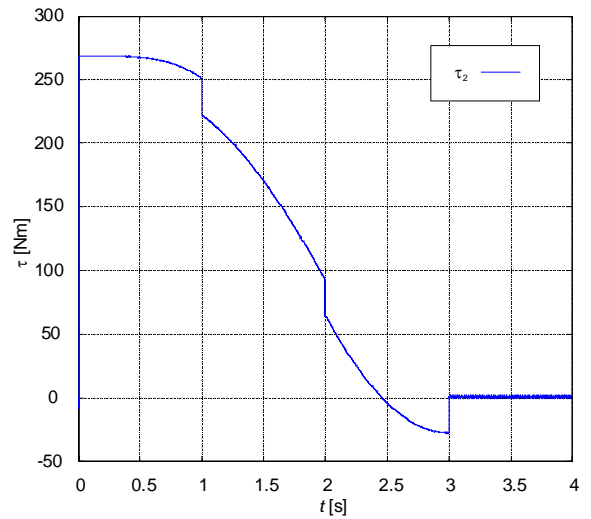


Fig. 13. Second link, stretched arm: driving torque τ_2

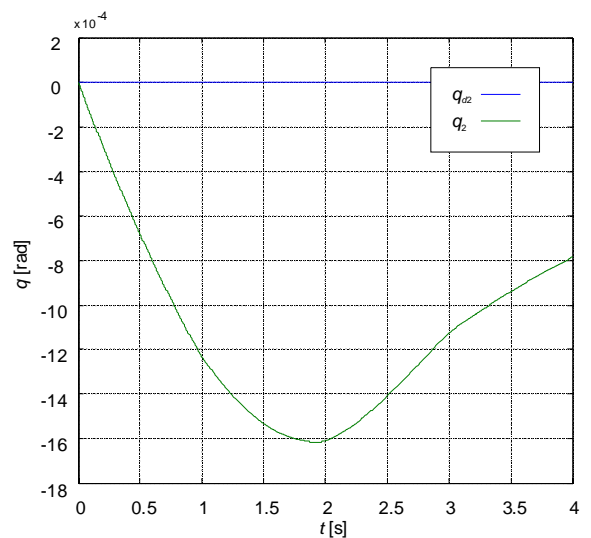


Fig. 14. Second link, stretched arm, detailed view: desired position q_{d2} and link position q_2

Notice the zero value of driving torques in steady state in Figures 10 and 13. This is the consequence of the vertical final position of the stretched link pair and therefore the zero influence of the gravitational forces. The wide interval of the driving torque variation in the second DOF, mirroring the torque in the first joint in spite of the constant mutual position between the links, shows the influence of the first link motion to the second link and proves the robustness of the control algorithm.

5. CONCLUSIONS

In this paper, the robustness and accuracy of a motion control algorithm based on the VSC theory – the equivalent time sub-optimal control – is verified and illustrated by the numerical simulation of a multi-DOF control system. Both the dynamic (tracking) and the steady-state accuracy have been achieved despite the enormous influence of the mechanical coupling among the DOF's of the robot manipulator. It has been demonstrated, that the proposed method assures the robustness against the signal as well as the parametric disturbances. The key to this method is the sliding mode control combined with the reaching law approach. The simple implementation of the control algorithm, given by the linear combination of the mechatronic system's straightforwardly accessible phase variables, represents an additional benefit of the presented method.

ACKNOWLEDGMENTS

The work presented in this contribution has been supported by the Grant Agency of Ministry of Education and Academy of Science of Slovak Republic VEGA under Grant No. 1/0690/09.

REFERENCES

- Hung, J.Y., W. Gao and J.C. Hung (1993). Variable Structure Control: A Survey. *IEEE Transactions on Industrial Electronics* **40**, 2-22.
- Kardoš, J. (2005). Reaching law modification of the time sub-optimal variable structure control. *International Journal of Mechanics and Control* **6**, 39-49.
- Kardoš, J. (2007). *Theory of Variable Structure Systems and the Time Sub-Optimal Control* (in Slovak). HMH Press. Bratislava.
- Kardoš, J. (2009). Variable structure motion control systems (in Slovak). *Automatizace* **52**, 688-692.
- Kardoš, J. (2010). The Simplified Dynamic Model of a Robot Manipulator. *Proceedings of the 18th International Conference – Technical Computing Bratislava 2010*. Bratislava.
- Utkin, V.I. (2002). First Stage of VSS: People and Events. In: *Variable Structure Systems: Towards the 21st Century* (X. Yu and J.X. Xu, Ed.). pp. 1-32. Springer Verlag. Berlin.
- Utkin, V.I., J. Guldner and J. Shi (1999). *Sliding Mode Control in Electromechanical Systems*. Taylor & Francis. London.